RUB-TP2-11/03

Leading twist coherent diffraction on nuclei in deep inelastic scattering at small x and nuclear shadowing

L. FRANKFURT
Nuclear Physics Dept., School of Physics and Astronomy, Tel Aviv University, 69978 Tel Aviv, Israel

V. GUZEY
Institut für Theoretische Physik II, Ruhr-Universität Bochum, D-44780 Bochum, Germany

M. STRIKMAN
Department of Physics, the Pennsylvania State University, State College, PA 16802, USA

Abstract

We extend the theory of leading twist nuclear shadowing to calculate leading twist nuclear diffractive parton distribution functions (nDPDFs). We observe that the quark and gluon nPDFs have different patterns of the A-dependence. It is found that the probability of diffraction in the quark channel increases with A, reaching about 30% at $x \sim 10^{-4}$ for $A \sim 200$, and weakly decreases with Q^2. In the gluon channel, the probability of diffraction is large for all nuclei ($\sim 40\%$ for heavy nuclei at $x \sim 10^{-4}$ and $Q_0^2 \sim 4$ GeV^2), it weakly depends on A and it decreases rather fast with increasing Q^2 – the probability decreases by approximately a factor of two as Q^2 changes from 4 GeV^2 to 100 GeV^2. We also find that nuclear shadowing breaks down Regge factorization of nDPDFs, which is satisfied experimentally in the nucleon case. All these novel effects in nDPDFs are large enough to be straightforwardly measured in ultraperipheral collisions at the LHC.

1 Introduction

It is firmly established by the HERA H1 [1, 2] and ZEUS [3] experiments that inclusive diffraction constitutes a significant fraction, about 10%, of the total cross section for deep inelastic scattering (DIS) of leptons on hydrogen. The diffractive events are characterized by the absence of hadronic activity in the detector at central rapidities. This QCD phenomenon involves both nonperturbative and perturbative aspects of the QCD dynamics, for the discussions see [4], and it is usually referred to as scattering off the "Pomeron". Note that in the case of DIS, the dynamics is quite different from that of the Pomeron pole exchange in soft hadron-hadron interactions, so we use the concept of Pomeron in order to indicate that we refer to the kinematics of large rapidity gaps and small momentum transfers to the recoil nucleon.

The proof of the factorization theorem for hard diffraction [5] enables one to describe the process in terms of Q^2-dependent diffractive parton distribution functions (DPDFs) and extract the DPDFs from various diffractive data. The current data [1, 2, 3] are consistent with the dominance of leading twist in hard diffraction and with the dominance of the gluon DPDF over the sum of the quark DPDFs. The DPDFs for the scattering off unpolarized

target, $f_{j/N}^{D(4)}(\beta, Q^2, x_{I\!P}, t)$ depend on four variables: Bjorken x, virtuality Q^2, four-momentum transfer squared to the target t and the fraction of the longitudinal momentum loss by the target $x_{I\!P}$.

The aim of the present paper is to investigate, within the leading twist approximation, nuclear dependence of coherent (without nuclear break-up) diffraction induced by hard probes and to obtain nuclear DPDFs. This would allow to calculate the cross sections of various diffractive DIS processes as well as of direct photon diffraction off nuclear targets. Experimental studies of these processes will be feasible in ultraperipheral collisions (UPC) of heavy ions at the LHC [6] and at the EIC [7].

Inclusive hard diffraction in DIS off nuclei has been studied in a number of papers, see e.g. [8, 9]. Unlike all previous attempts, we use the QCD factorization theorem for hard diffraction [5] and the leading twist theory of nuclear shadowing [10, 11, 12]. This enables us, for the first time, to calculate nDPDFs, i.e. to perform the flavor separation. This is an essential ingredient for the calculation of various, more complicated, problems such as charm production in DIS and dijet production in direct photon diffraction off nuclear targets, which need nDPDFs and especially the gluon nDPDF. The present paper complements our studies of the role of leading twist nuclear shadowing at small-x in inclusive processes with nuclei.

While we assume that the QCD factorization theorem for hard diffraction in DIS holds and all considered effects are leading twist effects, the studies of coherent diffraction on nuclei help to understand the transition to the regime of high parton densities. Indeed, the fraction of diffraction of the total cross section in DIS is a measure of how close to the black body regime (the regime of complete absorption of the projectile by the target) one is. While diffraction is approximately 10% of the total cross section in DIS on hydrogen, the fraction of diffractive events steadily increases as one increases the atomic number A, asymptotically approaching the absolute limit of one half.

This paper is structured as follows. In Sect. 2 we recapitulate essential points of the leading twist nuclear shadowing model and present the formula for coherent diffraction on nuclei. The analysis and discussion of the resulting expressions for nuclear diffractive parton distributions are presented in Sect. 3. We conclude and summarize in Sect. 4.

2 Leading twist nuclear shadowing and coherent diffraction on nuclei

The theory of leading twist nuclear shadowing is based on the Gribov's relation between nuclear shadowing and diffraction [14], Collins factorization theorem for hard diffraction in DIS [5] and the QCD analysis of the HERA data on hard diffraction in DIS on hydrogen [1, 2]. The foundations of the resulting theory and predictions for nuclear parton distribution functions and inclusive structure functions can be found in Refs. [10, 11, 12].

The master equation for the evaluation of the shadowing correction, $\delta f_{j/A}$, to the nuclear structure parton distribution functions of flavor j, $f_{j/A} = A f_{j/N} - \delta f_{j/A}$ has the form

$$\delta f_{j/A}(x,Q_0^2) = \frac{A(A-1)}{2} 16\pi \mathcal{R}e\Bigg[\frac{(1-i\eta)^2}{1+\eta^2}\int d^2b \int_{-\infty}^{\infty} dz_1 \int_{z_1}^{\infty} dz_2 \int_x^{x_{I\!P,0}} dx_{I\!P}$$
$$\times f_{j/N}^{D(4)}(\beta,Q_0^2,x_{I\!P},t_{\min})\rho_A(b,z_1)\rho_A(b,z_2) e^{ix_{I\!P} m_N (z_1-z_2)} e^{-(A/2)(1-i\eta)\sigma_{\rm eff}^j \int_{z_1}^{z_2} dz \rho_A(b,z)}\Bigg], \quad (1)$$

with η the ratio of the real to imaginary parts of the diffractive scattering amplitude; z_1, z_2 and $\vec{b}$ the longitudinal (in the direction of the incoming virtual photon) and transverse coordinates of the nucleons involved (defined with respect to the nuclear center); β, $x_{I\!P}$ and t the usual kinematic variables used in diffraction; $\beta = x/x_{I\!P}$; $t_{\min} \approx 0$; $\rho_A(b,z_i)$ the nucleon distribution in the target nucleus. The upper limit of integration, $x_{I\!P,0}$ is a cut-off parameter, which equals 0.1 for quarks and 0.03 for gluons. The effective cross section, $\sigma_{\rm eff}^j$, is expressed through the nucleon DPDFs as (see Ref. [12] for the detailed discussion and numerical estimates)

$$\sigma_{\rm eff}^j(x,Q_0^2) = \frac{16\pi}{f_{j/N}(x,Q_0^2)(1+\eta^2)} \int_x^{x_{I\!P,0}} dx_{I\!P} f_{j/N}^{D(4)}(\beta,Q_0^2,x_{I\!P},t)|_{t=t_{\min}}\,. \quad (2)$$

Equation (1) serves to define the input nuclear PDFs at the initial scale Q_0^2, $Q_0^2 = 4$ GeV^2 in our analysis. Nuclear PDFs at larger scales Q^2 are obtained using the NLO QCD evolution equations.

In Eq. (1), the interaction with two nucleons is calculated in a model-independent way. The only source of model-dependence is due to the approximation of the interaction with three and more nucleons by the attenuation factor $e^{-(A/2)(1-i\eta)\sigma_{\rm eff}^j \int_{z_1}^{z_2} dz \rho_A(b,z)}$, which involves $\sigma_{\rm eff}^j$, the rescattering cross section given by Eq. (2). While this quasi-eikonal approximation is expected to be valid at $Q_0^2 = 4$ GeV^2, it becomes progressively worse with increasing Q^2. The reason for this is that the eikonal approximation conserves the number of bare particles and thus contradicts QCD evolution. As a result, one obtains a wrong, higher twist, Q^2-dependence of nuclear shadowing in the processes dominated by small partonic configurations of the incoming virtual photon. Only at low Q^2 scales, where the effects of QCD evolution are not very important, can one justify the use of the eikonal and quasi-eikonal approximations. This means that Eq. (1) should be used only at the initial scale $Q_0^2 = 4$ GeV^2.

The generalization to the case of coherent diffraction in DIS on nuclei is rather straightforward, and it follows closely the case of the vector meson diffraction, see e.g. [15]. The nuclear diffractive parton distribution of flavor j can be presented in the form

$$f_{j/A}^{D(3)}(x,Q_0^2,x_{I\!P}) = \frac{A^2}{4} 16\pi f_{j/N}^{D(4)}(x,Q_0^2,x_{I\!P},t_{\min}) \int d^2b$$
$$\times \left|\int_{-\infty}^{\infty} dz e^{ix_{I\!P} m_N z} e^{\sigma_{\rm eff}^j A(1-i\eta)/2 \int_z^{\infty} \rho_A(b,z')} \rho_A(b,z)\right|^2 . \quad (3)$$

The superscripts (3) and (4) denote the dependence on three and four variables, respectively. We present our Eq. (3) for the t-integrated nuclear DPDFs since it is more compact and since it is not feasible to measure t in diffraction off nuclei in the collider experiments. In deriving

Eq. (3) we neglected a possible β-dependence of $\sigma^j_{\rm eff}(x,Q^2)$ in the exponential factor and substituted $\sigma^j_{\rm eff}$ by its average value. Since the total probability of diffraction changes rather weakly with $\sigma^j_{\rm eff}$, see e.g. [16], this seems a reasonable first approximation. At the same time, in the region of small β and small x corresponding to the triple Pomeron kinematics for soft inelastic diffraction, we expect a significant suppression of diffraction as compared to the quasi-eikonal approximation of Eq. (3) for $Q^2 \sim Q_0^2$, see the discussion in the end of the section.

One should note that the large momentum transfer Q^2, which is necessary for the applicability of the QCD factorization theorem, does not preclude the existence of coherent nuclear diffraction. Indeed, at high energies, the minimal momentum tranfer to the nucleus $t_{\rm min}$ is small, $t_{\rm min} \approx x_{Bj}^2 M_A^2$, which makes it possible for nucleus to stay intact (or diffract into low mass excited states). In practice, coherent nuclear diffraction can be identified by its distinctly sharp t-dependence in the forward direction (forward diffractive peak), which originates from the factor $\left(F_A(t)\right)^2$ where $F_A(t)$ is the nuclear form factor.

Assuming the exponential t-dependence of inclusive diffraction on free nucleons and using that $t_{\rm min} \approx 0$, we obtain

$$f^{D(4)}_{j/N}(x,Q_0^2,x_{I\!P},t=0) = B_j\, f^{D(3)}_{j/N}(x,Q_0^2,x_{I\!P})\,, \tag{4}$$

where B_j is a slope. In our analysis, we use $B_j = 7.2$ GeV^{-2} for quarks and $B_j = 6 + 0.25\ln(10^{-3}/x)$ GeV^{-2} for gluons, which are rather close numerically.

For sufficiently small values of $x_{I\!P}$, $x_{I\!P} \leq 0.01$, the H1 data [1, 2] and ZEUS data [3] can be fitted reasonably well using a factorized approximation first suggested within the picture of soft mechanism of diffractive process by Ingelman and Schlein [17]. In this approach, DPDFs can be presented as a product of a factor depending only on t and $x_{I\!P}$ (Pomeron flux) and a factor depending only on $\beta = x/x_{I\!P}$ and Q^2 (which is often referred to as the DPDF of the Pomeron)

$$f^{D(3)}_{j/N}(x,Q_0^2,x_{I\!P}) = f_{I\!P/p}(x_{I\!P})\, f_{j/I\!P}(\beta = x/x_{I\!P},Q_0^2)\,, \tag{5}$$

where $f_{I\!P/p}$ is the so-called Pomeron flux and $f_{j/I\!P}$ is the parton distribution function of the Pomeron.

Note that the QCD fits to the diffractive data lead to $\alpha_{I\!P}(0)$ for the effective Pomeron trajectory, which is somewhat larger than the one for the effective soft Pomeron trajectory. This is likely due to a different interplay of soft and semihard physics in hard diffraction at the Q_0^2 scale and a different role of screening compared to soft interactions. Hence, it is likely that a violation of the factorization approximation will be be observed once the data are more accurate.

The final expression for $f^{D(3)}_{j/A}$ takes the form

$$\begin{aligned} f^{D(3)}_{j/A}(x,Q_0^2,x_{I\!P}) &= \frac{A^2}{4} 16\pi B_j f_{I\!P/p}(x_{I\!P})\, f_{j/I\!P}(\beta = x/x_{I\!P},Q_0^2) \int d^2b \\ &\times \left| \int_{-\infty}^{\infty} dz e^{i x_{I\!P} m_N z} e^{\sigma^j_{\rm eff} A(1-i\eta)/2 \int_z^\infty \rho_A(b,z')} \rho_A(b,z) \right|^2 . \end{aligned} \tag{6}$$

One immediately sees from Eq. (6) that the factorization approximation is not valid for nuclear diffractive parton distributions, even if it is valid for the nucleon case: At fixed $x_{I\!P}$,

the right hand side of Eq. (6) depends not only on β but also on the Bjorken x since the screening factor is given by the exponential factor containing $\sigma^j_{\rm eff}$, which is a function of x. In addition, the right hand side of Eq. (6) depends on the atomic mass number A since the effect of nuclear shadowing increases with increasing A.

The aforementioned breakdown of the factorization approximation is a result of the increase of the nuclear shadowing effects both with the increase of incident energy and with the increase of the atomic number. This precludes the possibility of a scenario offered in Ref. [18], where coherent diffraction in DIS on nucleon and nuclear targets is provided by the same universal diffractive PDFs –"a universal Pomeron".

It is also worth noting that the approximation which we use at Q_0^2 in order to take into account multiple rescatterings, corresponds essentially to treating diffraction as superposition of elastic scattering of different components of the photon wave function off the nucleus. This is a reasonable approximation for the configurations with masses comparable to Q^2. As one approaches the $\beta \ll 1$ limit (which corresponds to $M_X^2 \gg Q^2$, one approaches the limit analogous to the soft triple Pomeron limit, in which case diffraction off nuclei is strongly suppressed as compared to the elastic scattering, see e.g. [8, 19]. This effect should be even stronger in our case of DIS since $\sigma^j_{\rm eff}$ increases with the decrease of β. Hence, we somewhat overestimate diffraction at small β and at relatively small Q_0^2 scale, see Figs. 2 and 3. At larger Q^2, diffraction at small β is dominated by the QCD evolution from $\beta \geq 0.1$ at Q_0^2 and, hence, the accuracy of our approximation improves. Hence, in the numerical studies, we neglect the effect of the small-β suppression.

3 Numerical results

In our analysis of Eq. (6), we used the 1994 H1 fit [1] for $f_{j/I\!P}$, where the gluon distribution is decreased by the factor 0.75. This change seems to be required by the more recent analysis of the 1997 H1 data on inclusive diffraction on hydrogen [2].

In order to have an idea about the magnitude of diffraction in DIS on hydrogen, the ratios $R_{j/N} \equiv f^{D(2)}_{j/N}/f_{j/N}$ for u-quarks and gluons and $F^{D(2)}_{2N}/F_{2N}$ are presented in Fig. 1 as functions of Bjorken x. Note that by definition

$$f^{D(2)}_{j/N}(x,Q^2) = \int_x^{x_{I\!P,0}} dx_{I\!P}\, f^{D(3)}_{j/N}(x,Q^2,x_{I\!P})\,. \tag{7}$$

These ratios give the probability of diffraction in the processes dominated by the coupling of a hard probe to a quark or gluon, respectively. For the hard process with a specific trigger, the probability of diffraction maybe close to $R_{q/N}$, such as the measurement of the diffractive structure function F^D_{2N}, or to $R_{g/N}$, such as the b-quark production. Alternatively, the probability of diffraction can have an intermediate value between $R_{q/N}$ and $R_{g/N}$, such as in the s-quark production. In Fig. 1, the solid curves correspond to $Q = 2$ GeV; the dashed curves correspond to $Q = 10$ GeV; the dot-dashed curves correspond to $Q = 100$ GeV. Since the Q^2 dependence of $g^{D(2)}_N/g_N$ is rather strong, we also show the ratio $g^{D(2)}_N/g_N$ at $Q = 5$ GeV (dotted curve). One sees from Fig. 1 that in the quark channel, diffraction constitutes 15-20% of the total cross section, while in the gluon channel diffraction is significantly larger [10]. This is likely to be related to a larger cross section of the interaction of the gluon color dipole (in the **8x8** representation) as compared to the triplet quark-antiquark dipole.

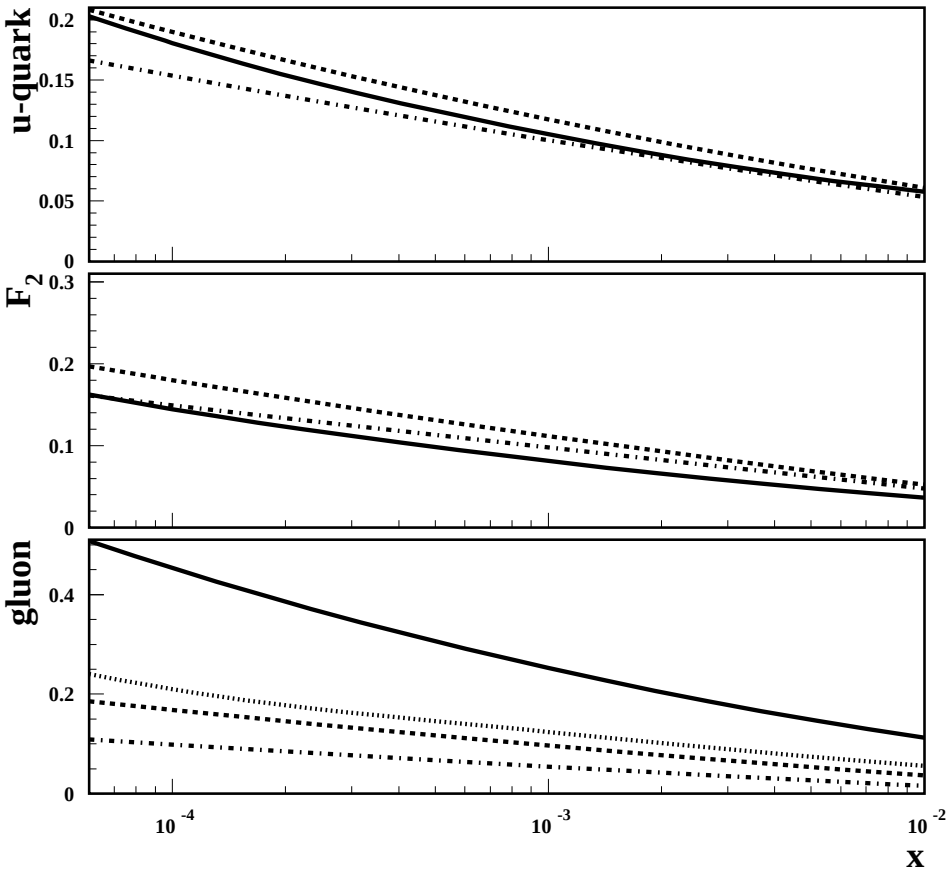

Figure 1: The ratios $f_{j/N}^{D(2)}/f_{j/N}$ for the u-quarks and gluons and NLO $F_{2N}^{D(2)}/F_{2N}$. The solid curves correspond to $Q = 2$ GeV; the dashed curves correspond to $Q = 10$ GeV; the dot-dashed curves correspond to $Q = 100$ GeV. In addition, for the gluons the dotted curve correspond to $Q = 5$ GeV.

The absolute upper limit of the gluon distribution, $g_N^{D(2)}/g_N = 1/2$ is reached at $x = 6 \times 10^{-5}$ and $Q = 2$ GeV. Since we prefer to stay away from modeling the kinematics, where taming of the increase of the diffractive parton distributions becomes necessary, we will consider the limited range of Bjorken x, $x > 6 \times 10^{-5}$, in this paper.

Next it is natural to analyze how the ratios presented in Fig. 1 change when hydrogen is replaced by a nuclear target. This can be done in two steps. First, acting in the spirit of the QCD factorization theorem for hard diffraction in DIS, Eq. (6) is used to define the input for DGLAP evolution at fixed $x_{I\!P}$. Subsequent QCD evolution enables us to determine $f_{j/A}^{D(3)}(x, Q^2, x_{I\!P})$ as a function of $\beta = x/x_{I\!P}$ and Q^2 at all fixed $x_{I\!P}$. An example of these results in presented in Figs. 2 and 3 for the nuclear targets of ^{40}Ca and ^{208}Pb. The u-quark and gluon nuclear diffractive parton distributions $f_{j/A}^{D(3)}(x, Q^2, x_{I\!P})$ (arbitrary absolute normalization) are presented as functions of $\beta = x/x_{I\!P}$ at two fixed values of $x_{I\!P} = 10^{-4}$

and $x_{I\!P} = 10^{-2}$. The solid curves correspond to $Q = 2$ GeV; the dashed curves correspond to $Q = 10$ GeV; the dot-dashed curves correspond to $Q = 100$ GeV; the dotted curves correspond to $Q = 5$ GeV. Different shapes and sizes of $f_{j/A}^{D(3)}(x, Q^2, x_{I\!P})$ at $x_{I\!P} = 10^{-4}$ and $x_{I\!P} = 10^{-2}$ clearly demonstrate violation of the factorization approximation for nuclear DPDFs.

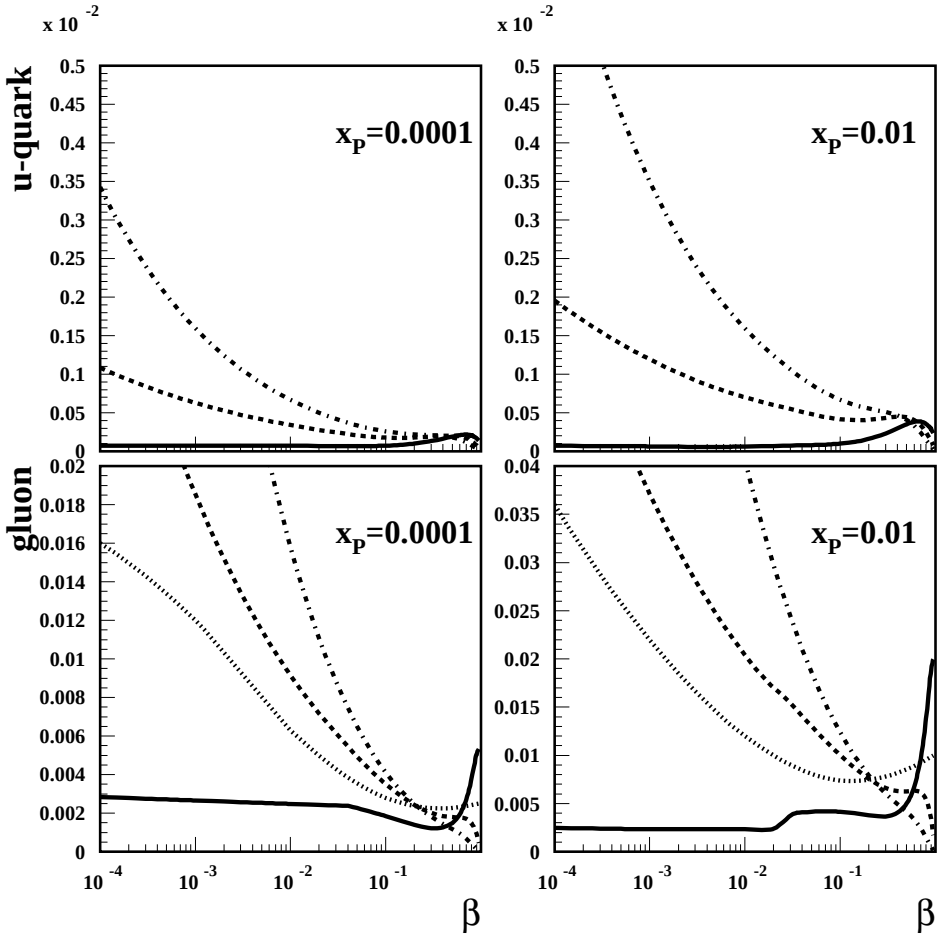

Figure 2: The u-quark and gluon nuclear (^{40}Ca) diffractive parton distribution as a function of β at two fixed values of $x_{I\!P}$. The solid curves correspond to $Q = 2$ GeV; the dashed curves correspond to $Q = 10$ GeV; the dot-dashed curves correspond to $Q = 100$ GeV. In addition, for the gluons the dotted curve correspond to $Q = 5$ GeV.

Another characteristic feature of nuclear DPDFs is that, like in the case of the free proton target, the gluon distribution is significantly larger than the quark distribution. However, we point out that the ratio of the quark to the gluon DPDF is significantly larger in the nuclear case because of a faster increase of the quark nDPDF with the atomic number A. Also, similarly to the free proton case, scaling violations of nDPDFs at large β are rather insignificant. This point is exemplified in Fig. 4 where we plot the u-quark and gluon nDPDFs as functions of Q^2 at fixed large $\beta = 0.5$ and small $x_{I\!P} = 10^{-3}$. One readily sees from Fig. 4

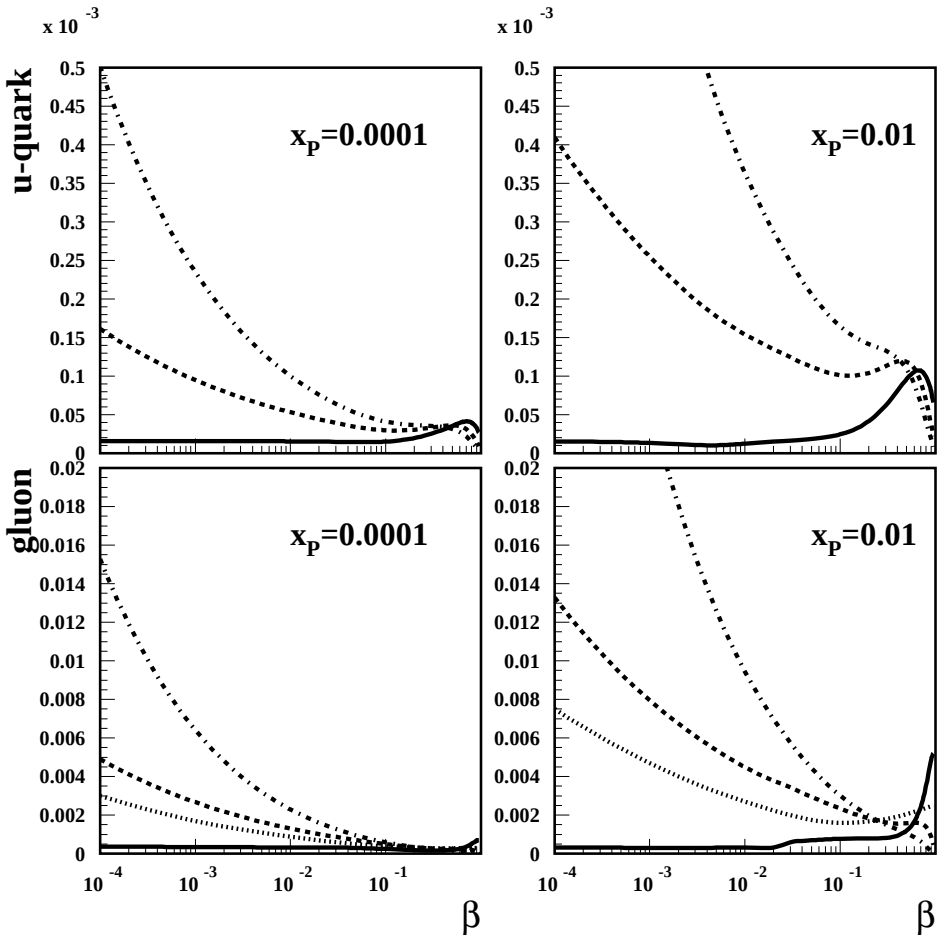

Figure 3: The u-quark and gluon nuclear (^{208}Pb) diffractive parton distribution as a function of β at two fixed values of $x_{I\!P}$. The solid curves correspond to $Q = 2$ GeV; the dashed curves correspond to $Q = 10$ GeV; the dot-dashed curves correspond to $Q = 100$ GeV. In addition, for the gluons the dotted curve correspond to $Q = 5$ GeV.

that QCD evolution in $\ln Q^2$ is weak.

The difference in large-β scaling violations of the structure function $F_2^{D(3)}$ in the nuclear and nucleon case is presented in Fig. 5. At $x_{I\!P} = 10^{-3}$ and two values of β, $\beta = 0.5$ and $\beta = 0.1$, $F_2^{D(3)}$ is plotted as a function of Q^2 for ^{40}Ca (solid curves), ^{208}Pb (dashed curves) and free nucleon (dot-dashed curves). The curves are normalized to coincide at the lowest $Q^2 = 4$ GeV^2. One can readily observe from Fig. 5 that scaling violations are largest for the free nucleon and that scaling violations decrease as one increases A.

Having obtained $f_{j/A}^{D(3)}(x, Q^2, x_{I\!P})$, they can be integrated over over $x_{I\!P}$ at fixed Bjorken x, just like in Eq. (7). The resulting $f_{j/A}^{D(2)}/f_{j/A}$ ratios for the u-quarks and gluons and NLO $F_{2A}^{D(2)}/F_{2A}$ are presented in Fig. 6 for ^{40}Ca and in Fig. 7 for ^{208}Pb. From Figs. 6 and 7 one can see that the fraction of the diffractive events in DIS at small x for moderately heavy

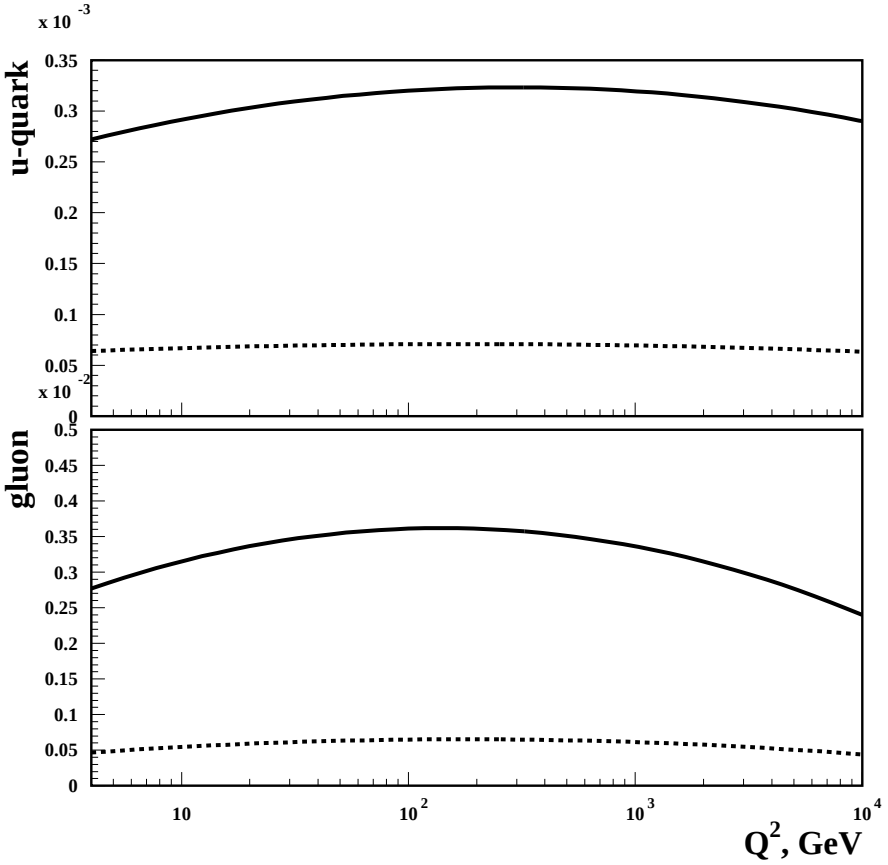

Figure 4: The u-quark and gluon nuclear PDFs as functions of Q^2 at $\beta = 0.5$ and small $x_{I\!P} = 10^{-3}$. The solid curves correspond to ^{40}Ca; the dotted curves correspond to ^{208}Pb.

and heavy nuclei is of the order of 30% and weakly changes with Q^2, which is in a good agreement with the early estimates of Ref. [8]. In the case of gluon-induced reactions, the probability decreases rather significantly with an increase of Q^2. However, the probability still remains at the level of 15-20% at $Q = 10$ GeV and, hence, it would be feasible to study this in ultraperipheral collisions at the LHC using, for instance, production of heavy flavors similarly to the case of inclusive production considered in [20]. Another option is to use dijet production like it was done in the proton case in the ZEUS [21] and H1 [2] experiments.

Another conclusion that can be drawn from Figs. 6 and 7 is that the A-dependence of the probability of coherent diffraction is rather weak for $A \geq 40$. For these values of A, the interaction for the central impact parameters is close to being completely absorptive (black) with a small contribution from the opaque nuclear edge. Moreover, the A-dependence is weaker in the gluon case since the gluon interactions at the Q_0 scale are already close to the black limit, even for the nucleon.

Mathematically this pattern is a result of a compensation of two effects – stronger small-x nuclear shadowing in the case of coherent diffraction compared to the inclusive case, is compensated by the nuclear form factor, as a consequence of nuclear coherence.

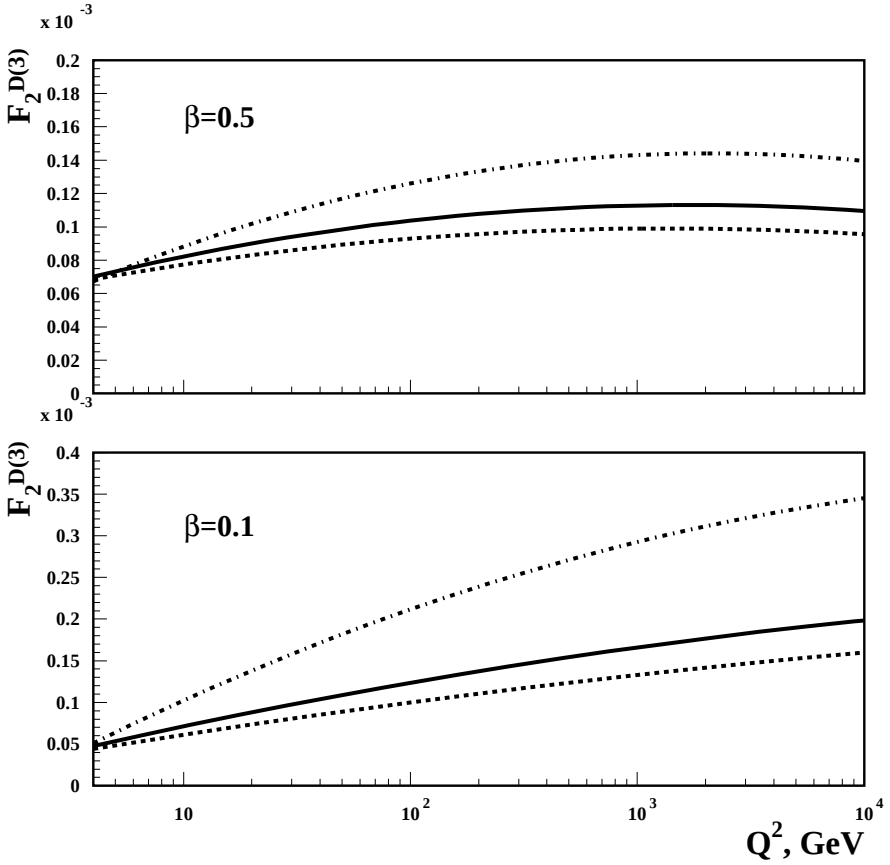

Figure 5: The diffractive structure function $F_2^{D(3)}$ as a function of Q^2 at $\beta = 0.5$ and $\beta = 0.1$ and small $x_{I\!P} = 10^{-3}$. The solid curves correspond to ^{40}Ca; the dotted curves correspond to ^{208}Pb; the dot-dashed curves correspond to the free nucleon.

It is worth noting a qualitative difference between the A-dependence of the fraction of the diffractive events in the quark and gluon-induced processes at small x. In the gluon case, it is a very weak function of A because already in the proton case, the probability of diffraction is close to one half, the maximal value allowed by unitarity. At the same time in the quark case a steady growth with A is predicted since for the proton the probability of diffraction in this channel is rather small and, hence, the increase of the blackness of the interaction with A leads to a gradual increase of the diffraction probability to the values close enough to the black body limit.

4 Conclusions and Discussion

We study small-x coherent diffraction in DIS on nuclear targets using the theory of leading twist nuclear shadowing and the QCD factorization theorem for hard diffraction. It is demonstrated that Bjorken x and A-dependent nuclear shadowing explicitly breaks down

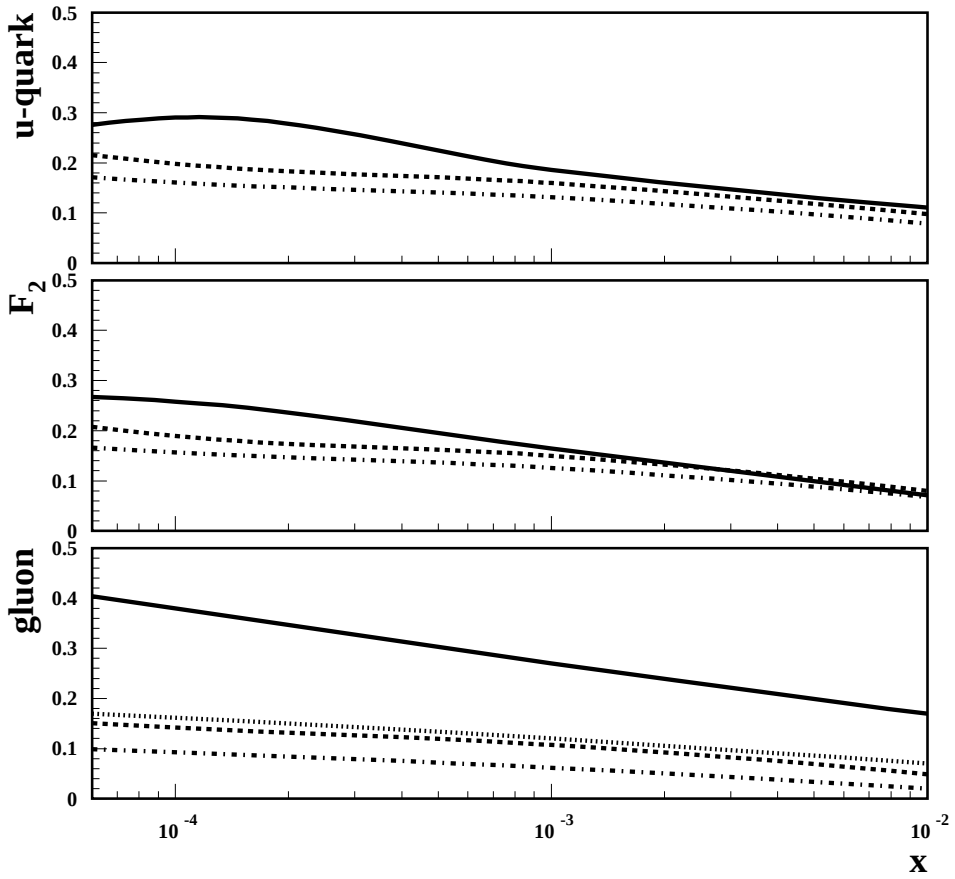

Figure 6: The ratios $f_{j/A}^{D(2)}/f_{j/A}$ for the u-quarks and gluons and NLO $F_{2A}^{D(2)}/F_{2A}$ for ^{40}Ca. The solid curves correspond to $Q = 2$ GeV; the dashed curves correspond to $Q = 10$ GeV; the dot-dashed curves correspond to $Q = 100$ GeV. In addition, for the gluons the dotted curve correspond to $Q = 5$ GeV.

Regge factorization in diffraction, which means that at fixed $x_{I\!P}$, nuclear parton distribution functions depend not only on $\beta = x/x_{I\!P}$ but also on Bjorken x and A.

We calculate nuclear DPDFs (Figs. 2, 3 and 4) as functions of β, Q^2, $x_{I\!P}$ and the atomic number A. Like in the free nucleon case, the gluon nDPDF is much larger than the quark nDPDF. Using the calculated nDPDFs, the contribution of coherent diffraction to the total probability is estimated for the u-quark and gluon channels as well as for the NLO F_2 structure functions (Figs. 6 and 7). The key result is an observation of dramatically different patterns of the A-dependence. In the quark channel and in the F_2 case, the probability of diffraction increases with A, reaching about 30% at $x \sim 10^{-4}$ and $Q_0^2 \sim 4$ GeV^2 and for $A \sim 200$. In the gluon channel, the probability of diffraction is already large for the proton and, hence, it changes (decreases) rather insignificantly when the proton target is replaced by the heavy nuclear target: the probability remains at the level of $\sim 40\%$ at $x \sim 10^{-4}$ and

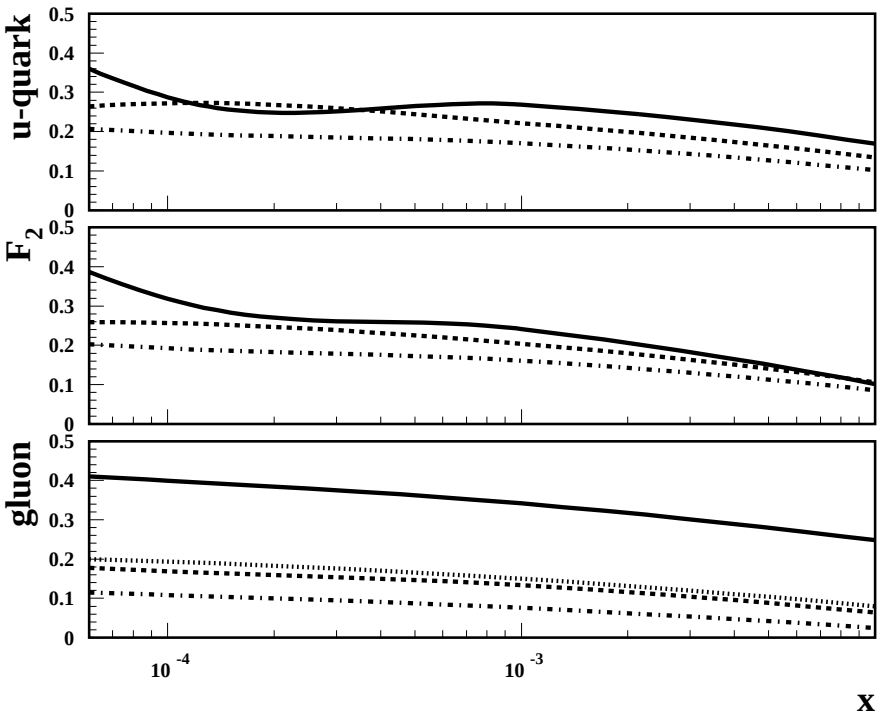

Figure 7: The ratios $f_{j/A}^{D(2)}/f_{j/A}$ for the u-quarks and gluons and NLO $F_{2A}^{D(2)}/F_{2A}$ for ^{208}Pb. The solid curves correspond to $Q = 2$ GeV; the dashed curves correspond to $Q = 10$ GeV; the dot-dashed curves correspond to $Q = 100$ GeV. In addition, for the gluons the dotted curve correspond to $Q = 5$ GeV.

$Q_0^2 \sim 4$ GeV^2.

The Q^2-dependence of the probability of diffraction is also different in the quark and the gluon channels. The very large gluon diffractive distribution makes QCD evolution of the ratios $u_A^{D(2)}/u_A$ and NLO $F_{2A}^{D(2)}/F_{2A}$ rather weak. At the same time, the ratio $g_A^{D(2)}/g_A$ falls off rapidly as Q^2 increases (compare the solid and broken curves in Figs. 6 and 7).

From the experimental point of view, coherent diffraction in deep inelastic scattering on nuclei can be identified via a two-step procedure. First, similarly to the case of ep scattering, one selects events with a rapidity gap. Second, one needs to separate the coherent and incoherent diffraction. This can be readily done using the lack of neutrons in the zero angle neutron calorimeter since the break-up of the nucleus in incoherent diffraction results in production of several evaporation neutrons, see discussion in [18]. In addition, the ratio of incoherent diffraction to coherent diffraction is expected to be $\sim 0.1-0.15$ [16]. Hence overall

in the collider kinematics the task of selecting the diffractive channel without break-up of the target appears to be much easier in the nucleus case than in the proton case. The t-dependence of coherent diffraction originates primarely from the factor $(F_A(t))^2$ where $F_A(t)$ is the nuclear form factor. Hence average t are small and it is hardly possible to measure the t-dependence of the diffractive amplitude for the case of the large masses of the produced diffractive system. However since the t-dependence is mostly trivial, inability to measure the differential cross section would not lead to a significant loss of information about the dynamics of diffraction. Note also that that the break-up channel originates mostly due to the scattering off the edge of the nucleus, leading to the same pattern of diffraction as in the scattering off a free nucleon. Hence we predict a different $\beta, x_{I\!P}, Q^2$ dependence of the hard diffraction in incoherent and coherent diffraction.

Nuclear diffractive PDFs, discussed in this paper, exhibit novel effects, which are large enough to be measured in the ultraperipheral collisions at the LHC. We also would like to emphasize that the proximity of the probability of hard diffraction to the unitarity limit at $Q^2 \sim 4$ GeV^2 shows that the color transparency phenomenon and related to Bjorken scaling decomposition over powers of $1/Q^2$, which are typical for DIS, disappear in the vicinity of these Q^2. Thus, nuclear shadowing does not preclude observation of a variety of phenomena characteristic for the unitarity limit for the gluon channel in the case of the nucleon and nuclear targets at $x \leq 10^{-3}$, and for the quark channel for $x \leq 10^{-4}$ for heavy nuclear targets. In particular, we expect that blackening of the interaction will reveal itself in heavy ion collisions at the LHC (and to less extent at RHIC) in the filtering out of nonperturbative QCD effects and producing a pQCD phase in the proton-nucleus collisions in the proton fragmentation region [22] and in the heavy ion collisions in the ion fragmentation regions [23].

Numerical results presented in this paper are available from V. Guzey (vadim.guzey@tp2.ruhr-uni-bochum.de) upon request.

This work was supported by Sofia Kovalevskaya Program of the Alexander von Humboldt Foundation (Germany) and Department of Energy (USA) and GIF.

References

[1] C. Adloff *et al.*, H1 Collab., Z. Phys. **C 76** (1997) 613.

[2] H1 Collab., 31st International Conference on High Energy Physics, ICHEP02, July 24, 2002, Amsterdam.

[3] J. Breitweg *et al.*, ZEUS Collab., Eur. Phys. J. **C 6** (1999) 43.

[4] *Future physics at HERA*, Proceedings of HERA workshop, Hamburg, Germany, Sept. 95-May 96, Eds. G. Ingelman, A. De Roeck and R. Klanner.

[5] J.C. Collins, Phys. Rev. **D 57** (1998) 3051; Erratum *ibid.* **D 61** (2000) 019902.

[6] Yellow Report on Ultraperipheral collisions, in preparation.

[7] The Electron Ion collider, White Paper, BNL-68933, February 2002.

[8] L.L. Frankfurt and M.I. Strikman, Phys. Lett. **B 382** (1996) 6.

[9] E. Levin and M. Lublinsky, Nucl. Phys. **A 712** (2002) 95.

[10] L. Frankfurt and M. Strikman, Eur. Phys. J. **A 5** (1999) 293.

[11] L. Frankfurt, V. Guzey, M. McDermott and M. Strikman, J. High Energy Phys. **202** (2002) 27.

[12] L. Frankfurt, V. Guzey, and M. Strikman, hep-ph/0303022.

[13] L. Frankfurt, G. A. Miller and M. Strikman, Phys. Lett. **B 304** (1993) 1 [hep-ph/9305228].

[14] V.N. Gribov, Sov. Phys. JETP **29** (1969) 483 [Zh. Eksp. Tor. Fiz. **56** (1969) 892].

[15] T.H. Bauer, R.D. Spital, D.R. Yennie and F.M. Pipkin, Rev. Mod. Phys. **50** (1978) 261.

[16] L. Frankfurt, M. Strikman and M. Zhalov, Acta Phys. Polon. **B 34** (2003) 3215.

[17] G. Ingelman and P. E. Schlein, Phys. Lett. **B 152** (1985) 256.

[18] M. Arneodo *et al.*, in Proceedings of Workshop on Future Physics at HERA, Eds. G. Ingelman, A. De Roeck and R. Klanner [hep-ph/9610423].

[19] A.B. Kaidalov *et al.*, Acta Phys. Polon. **B 34** (2003) 3163 [hep-ph/0303111].

[20] S. R. Klein, J. Nystrand and R. Vogt, Phys. Rev. **C 66** (2002) 044906 [hep-ph/0206220].

[21] M. Derrick *et al.* [ZEUS Collaboration], Phys. Lett. **B 356** (1995) 129 [hep-ex/9506009].

[22] A. Dumitru, L. Gerland and M. Strikman, Phys. Rev. Lett. **90** (2003) 092301 [hep-ph/0211324].

[23] L. Frankfurt and M. Strikman, Phys. Rev. Lett. **91** (2003) 022301 [nucl-th/0212094].